Angewandte Chemie

Accepted Article

This manuscript has been accepted after peer review and appears as an Accepted Article online prior to editing, proofing, and formal publication of the final Version of Record (VoR). The VoR will be published online in Early View as soon as possible and may be different to this Accepted Article as a result of editing. Readers should obtain the VoR from the journal website shown below when it is published to ensure accuracy of information. The authors are responsible for the content of this Accepted Article.

RESEARCH ARTICLE

Solar-driven Overproduction of Biofuels in Microorganisms

Jie Wang,[a],+ Na Chen,[a],+ Guangkai Bian,[a] Xin Mu,[a] Na Du,[a] Wenjie Wang,[b] Chong-Geng Ma,[d]

Shai Fu,[a] Bolong Huang,[c] Tiangang Liu,[a] Yanbing Yang,*,[a] Quan Yuan*,[a,b]

[a]   Dr. J. Wang+, N. Chen+, Dr. G. K. Bian, X. Mu, N. Du, S. Fu, Prof. T. G. Liu, Prof. Y. B. Yang, Prof. Q. Yuan
        College of Chemistry and Molecular Sciences
        Key Laboratory of Combinatorial Biosynthesis and Drug Discovery (Wuhan University), Ministry of Education
        School of Pharmaceutical Sciences
        Wuhan University, Wuhan, China
        E-mail: yuanquan@whu.edu.cn
        E-mail: yangyanbing@whu.edu.cn
[b]   W. Wang, Prof. Q. Yuan
        Molecular Science and Biomedicine Laboratory (MBL)
        State Key Laboratory of Chemo/Biosensing and Chemometrics
        College of Chemistry and Chemical Engineering
        Hunan University, Changsha, China
[c]   Prof. B. L. Huang
        Department of Applied Biology and Chemical Technology
        The Hong Kong Polytechnic University, Hung Hom, Kowloon, Hong Kong, China.
[d]   Prof. C.-G. Ma
        CQUPT-BUL Innovation Institute
        School of Optoelectronic Engineering
        Chongqing University of Posts and Telecommunications, Chongqing, China.

+   These authors contributed equally to this work.

        Supporting information for this article is given via a link at the end of the document.

Abstract: Microbial cell factories reinvigorate current industries by producing complex fine chemicals at low costs. Reduced nicotinamide adenine dinucleotide phosphate (NADPH) is the main reducing power to drive the biosynthetic pathways in microorganisms. However, the insufficient intrinsic NADPH limits the productivity of microorganisms. Here, we report that supplying microorganisms with long-lived electrons from persistent phosphor mesoporous Al_2O_3 (meso-Al_2O_3) can elevate the NADPH level to facilitate efficient fine chemicals production. The defects in meso-Al_2O_3 were demonstrated to be highly efficient in prolonging electrons' lifetime. The long-lived electrons in meso-Al_2O_3 can pass the material-microorganism interface and power the biosynthetic pathways of *E. coli* to produce jet fuel farnesene. This work represents a reliable strategy to design photo-biosynthesis systems to improve the productivity of microorganisms with solar energy.

Introduction

Tremendous advances in metabolic engineering and synthetic biology during the last 20 years have reinvigorated the energy, pharmaceutical, and chemical industries with microbial cell factories.[1] By reconstructing the desired metabolic pathways in microorganisms, microbial cell factories can produce complex fine chemicals including biofuels and pharmaceuticals at low costs.[2] The mevalonate (MVA) biosynthetic pathway is widely used in biosynthesis, through which a great diversity of isoprenoid-based fine chemicals[2b,3] including antimalarial drug artemisinin[4] and jet fuel farnesene[1c,5] have been produced. Biosynthetic pathways involve a series of redox reactions performed at the molecular level.[1a,1c,5,6] The reduced nicotinamide adenine dinucleotide phosphate (NADPH) is pivotal in these redox processes since it serves as the electron carrier for a large subset of

oxidoreductases in biosynthetic pathways.[7] The production of fine chemicals in microorganisms requires huge amounts of NADPH to drive the biosynthetic pathways.[6,8] However, the intrinsic NADPH in microorganisms is far from enough to drive the biosynthetic pathways.[6,8,9] The lack of NADPH is a major hurdle that limits the productivity of microbial cell factories,[7-10] including the MVA pathway for producing isoprenoid-based chemicals.[1c] Owing to the pivotal role of NADPH as the electron carrier, accelerating NADPH regeneration has long been of keen interest in improving the productivity of fine chemicals in microorganisms.

Previous studies have demonstrated that microorganisms are capable of accepting electrons from extracellular materials,[11] and the accepted electrons can be used to generate NADPH for powering the biosynthetic pathways.[12] Therefore, feeding microorganisms with extracellular electrons is a promising paradigm for facilitating NADPH generation and increasing the yields of fine chemicals production in the MVA biosynthetic pathway. Semiconductors are highly efficient in producing photo-excited electrons under illumination,[13] and the photo-excited electrons can serve as extracellular electrons to drive the biosynthesis processes in microorganisms. Whereas, the semiconductor-microorganism interface represents a barrier in the transfer of photo-excited electrons into microorganisms.[14] Ideally, photo-excited electrons with long enough lifetimes can pass through the semiconductor-microorganism interface more easily to reach the cytosolic NADPH regeneration reactions.[12c,15]

Defects are the disruption of the regular atoms in the crystal lattice.[16] Crystal defects can inhibit the annihilation of photo-excited electrons and supply channels for electron migration, which benefits the generation of photo-excited electrons with long lifetimes.[16] Motivated by the defects-mediated long lifetime electrons, here we demonstrated that supplying farnesene producing *E. coli* with long-lived extracellular electrons from

RESEARCH ARTICLE

persistent phosphors can significantly improve the cytosolic NADPH level and the farnesene production yield. Specifically, the catalytic machinery of the MVA pathway in engineered *E. coli* was integrated with mesoporous Al_2O_3 (meso-Al_2O_3) persistent phosphor for light-accelerated production of jet fuel farnesene (Figure 1). The defect density was largely increased by constructing a highly porous structure, which led to a significantly prolonged lifetime of the photo-excited electrons in defective meso-Al_2O_3. With the support of the long-lived electrons from the light-harvesting meso-Al_2O_3, the yield of farnesene in *E. coli* was increased from 900 mg/L to 1816 mg/L under visible light illumination. Gene knockout assays further suggested that c-type cytochrome and pili participated in the transfer of long-lived electrons from the defective meso-Al_2O_3 to *E. coli*. These findings provide an efficient strategy to prolong the lifetime of photo-excited electrons in solid materials and the developed hybrid photo-biosynthesis system furnishes an effective channel for solar-to-chemical production with microbial cell factories.
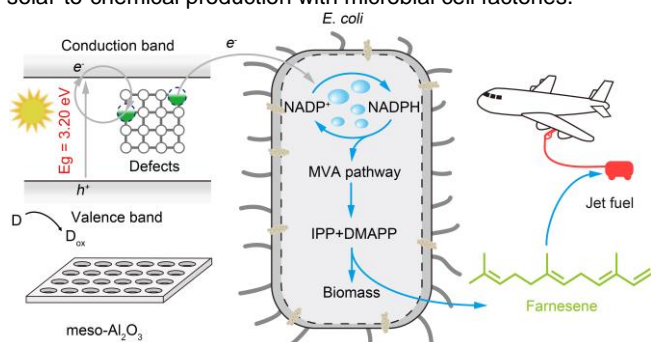

Figure 1. Schematic diagram of the hybrid photo-biosynthesis system for farnesene overproduction. The hybrid photo-biosynthesis system was constructed by adding mesoporous Al_2O_3 (meso-Al_2O_3) into the *E. coli* culture medium. The abundant defects in the meso-Al_2O_3 mediate the generation of long-lived electrons under visible light illumination. The long-lived electrons migrate into the *E. coli* to accelerate the regeneration of reduced nicotinamide adenine dinucleotide phosphate (NADPH). The elevated amount of NADPH powers the mevalonate (MVA) pathway to increase the yield of jet fuel farnesene. The isopentenyl pyrophosphate (IPP) and dimethylallyl pyrophosphate (DMAPP) are the universal C_5 precursors for the production of isoprenoid-based fine chemicals including farnesene. D, electron donors in the cell culture medium; D_{ox}, oxidized electron donor species.[10]

Results and Discussion

To provide farnesene producing *E. coli* with long-lived electrons for farnesene overproduction, defects were introduced in Al_2O_3 by mesoporous structure to prolong the lifetime of photo-excited electrons. The defective meso-Al_2O_3 displays uniform mesopores (Figure 2a, Figure S1 and S2) with an average pore diameter of about 8 nm (Figure S3 and Figure S4).[17] The defective features of the meso-Al_2O_3 and nonporous Al_2O_3 (np-Al_2O_3) were systematically investigated. The positron lifetime spectra of meso-Al_2O_3 and np-Al_2O_3 (Figure 2b) are well decomposed by LT routine into τ_1-τ_4 components (Table S1),[18] in which τ_3 represents spin-parallel orthopositronium (o-Ps) annihilation in the negatively charged defects. The τ_3 of o-Ps in defective meso-Al_2O_3 and np-Al_2O_3 is 1.27 ± 0.01 ns and 2.23 ± 0.07 ns, respectively. The

shorter τ_3 of o-Ps in meso-Al_2O_3 suggests the presence of large amounts of aluminum vacancies in defective meso-Al_2O_3. On the other hand, in electron paramagnetic resonance (EPR) spectroscopy, the defective meso-Al_2O_3 shows a remarkable symmetric absorption peak (Figure 2c) at around 326.7 mT. The g-factor of the EPR absorption line was calculated to be 2.011, indexing to electrons captured by oxygen vacancies.[19] In X-ray photoelectron spectroscopy (XPS) curves (Figure S5), the Al 2p peak of meso-Al_2O_3 shifts from 74.3 eV to 74.7 eV, further suggesting the presence of oxygen vacancies in defective meso-Al_2O_3. The EPR and XPS assays confirm the presence of larger quantities of oxygen vacancies in defective meso-Al_2O_3 compared with np-Al_2O_3. The positron lifetime spectra, EPR, and XPS analysis suggest that cationic and anionic defects can be efficiently created in materials by constructing a highly porous structure.

Generally, defects can serve as electronic transition intermediate states to narrow the bandgap of materials and mediate the transition of photo-excited electrons, which can extend the light absorption range of materials. The UV-Vis diffuse reflectance absorption spectra show that the meso-Al_2O_3 displays broad absorption in the visible region (inset in Figure 2d). The optical bandgap energy (Eg) of the meso-Al_2O_3 was calculated to be about 3.20 eV, confirming the visible light absorption capability of the defective meso-Al_2O_3. Compared to the np-Al_2O_3, the excitation band of meso-Al_2O_3 is significantly enhanced and red-shifts about 20 nm (Figure S6). Also, the meso-Al_2O_3 can be directly excited by visible light. These features make meso-Al_2O_3 suitable to harvest solar energy for accelerating the production of fine chemicals in microorganisms. The np-Al_2O_3 and meso-Al_2O_3 produce a broad emission across 320-580 nm (Figure 2e), which can be ascribed to the defects-related radiative centers in Al_2O_3 according to previous studies.[20] The maximum emission band of the defective meso-Al_2O_3 is red-shifted by about 30 nm compared to np-Al_2O_3, confirming the presence of abundant crystal defects-mediated transition intermediate states in the bandgap of the defective meso-Al_2O_3. The above results demonstrate that the optoelectronic properties of materials can be efficiently modified by introducing defects. In addition to narrowing the bandgap, defects can also serve as trap states to suppress charge recombination and extend the lifetime of electrons. The luminescence lifetime of defective meso-Al_2O_3 is determined to be about 165.4 ms (Figure 2f), clearly showing the existence of long-lived electrons in defective meso-Al_2O_3. Moreover, the meso-Al_2O_3 displays brighter and more durable persistent luminescence than the np-Al_2O_3 (Figure 2g, Figure S7, Video S1 and S2). The bright persistent luminescence in meso-Al_2O_3 originates from the gradual annihilation of the long-lived electrons with holes after excitation ceases. The pre-charged defective meso-Al_2O_3 displays strong emission bands at around 100 °C and 450 °C in thermally stimulated luminescence (TSL) spectra (Figure S8). The TSL bands are attributed to the annihilation of long-lived electrons trapped by crystal defects,[16c] which suggests that the abundant defects in meso-Al_2O_3 serve as trap states to prolong the lifetime of the electrons. These data thus support the conclusion that introducing defects into solid materials can efficiently prolong the lifetime of photo-excited electrons. The long-lived electrons in solid materials can be transported to microorganisms easier than the short-lived ones.
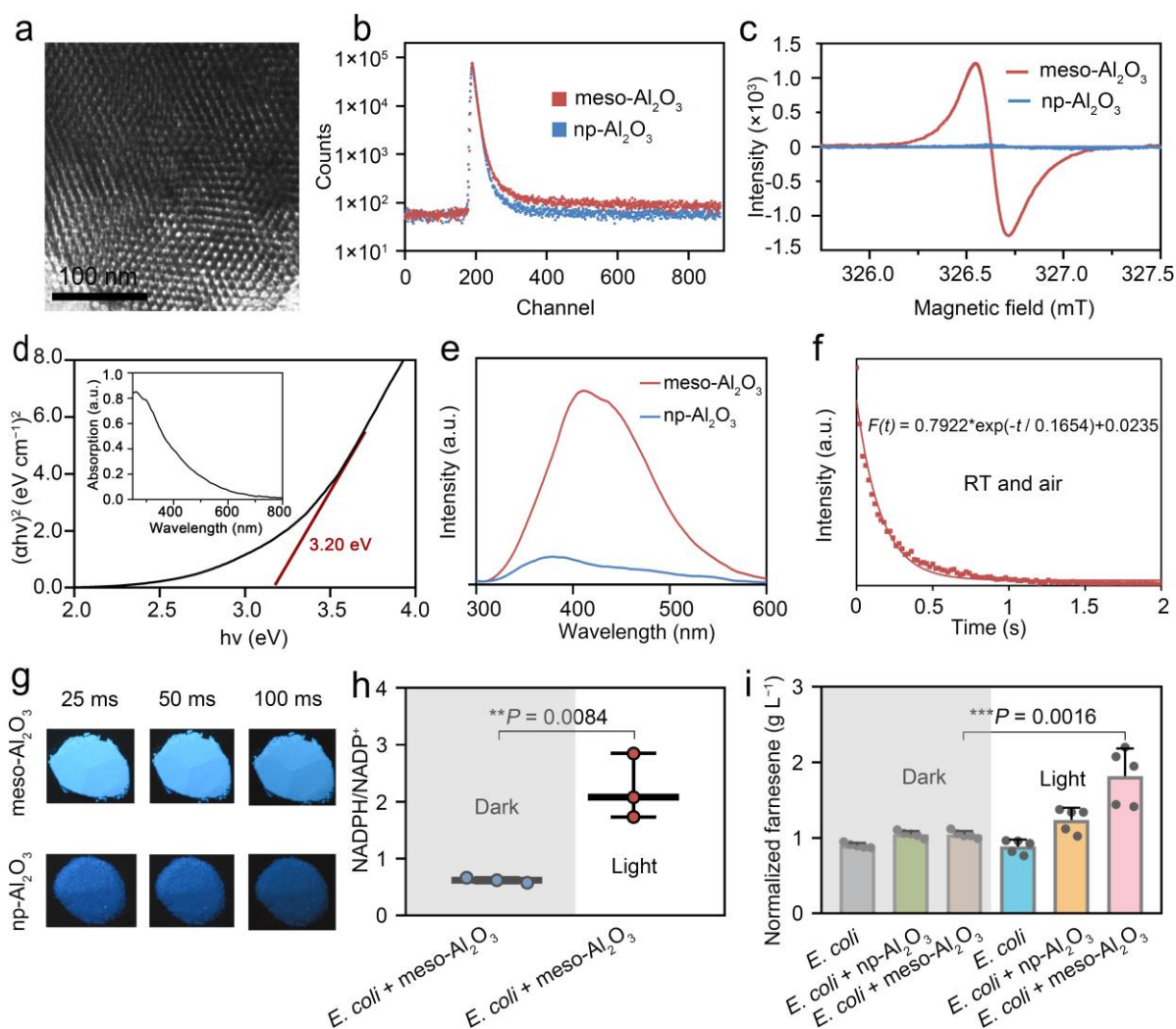
RESEARCH ARTICLE

Figure 2. Accelerated farnesene production by defective mesoporous Al_2O_3 (meso-Al_2O_3) under visible light illumination. (a) Transmission electron microscopy image of the defective meso-Al_2O_3. Positron lifetime spectra (b) and electron paramagnetic resonance spectra (c) of the defective meso-Al_2O_3 and nonporous Al_2O_3 (np-Al_2O_3). (d) Tauc plot of the meso-Al_2O_3. Inset: ultraviolet-vis diffuse reflectance absorption spectrum of the meso-Al_2O_3. (e) Photoluminescence spectra of the meso-Al_2O_3 and np-Al_2O_3. (f) Transient photoluminescence decay curve of the meso-Al_2O_3. RT, room temperature. (g) Persistent luminescence images of the defective meso-Al_2O_3 and np-Al_2O_3. (h) The ratio of reduced nicotinamide adenine dinucleotide phosphate to nicotinamide adenine dinucleotide phosphate (NADPH/NADP$^+$) in the meso-Al_2O_3/*E. coli* hybrid system at different conditions. (i) The amount of produced farnesene by bare farnesene producing *E. coli*, farnesene producing *E. coli* treated with np-Al_2O_3, and meso-Al_2O_3/*E. coli* hybrid system at different conditions. Error bars show the mean ± standard error of the mean (s.e.m.) of three or five independent measurements.

The performance of the defective meso-Al_2O_3 in supplying electrons for the production of NADPH and farnesene was further investigated. In transient photocurrent tests, the defective meso-Al_2O_3 produces a cathodic photocurrent 1.5 times higher than the np-Al_2O_3, showing the strong electron-donating ability of the defective meso-Al_2O_3 (Figure S9). Also, the efficient conversion of nicotinamide adenine dinucleotide phosphate (NADP$^+$) into NADPH in solution is observed in the presence of defective meso-Al_2O_3 and visible light illumination (Figure S10). Particularly, under the simulated solar light illumination, a significant increase in the typical absorbance of NADPH at 340 nm is observed, suggesting that the solar light-excited electrons in meso-Al_2O_3 could be used for NADPH generation (Figure S10). A step further, the engineered farnesene producing *E. coli* was constructed according to our previously reported protocol,[5] and the defective meso-Al_2O_3 was integrated with the engineered *E. coli* for farnesene production. As shown in Figure 2h, the NADPH/NADP$^+$ ratio in *E. coli* of the hybrid photo-biosynthesis system is more

than 2 times higher than that in bare engineered *E. coli*, clearly indicating that the electrons obtained from defective meso-Al_2O_3 can be used in the regeneration of NADPH in *E. coli*. To further validate the performance of defective meso-Al_2O_3 in accelerating the farnesene producing pathway, the yields of farnesene production in *E. coli* were quantified and presented in Figure 2i. In the absence of defective meso-Al_2O_3, the bare engineered *E. coli* produces a low amount of farnesene, about 900 mg/L, regardless of light illumination. In marked contrast, the amount of farnesene in the hybrid photo-biosynthesis system is 1816 mg/L, 2.02 times the farnesene produced by the bare engineered *E. coli* and 1.47 times the farnesene produced in the np-Al_2O_3/*E. coli* group. The significantly increased farnesene production in the hybrid meso-Al_2O_3/*E. coli* photo-biosynthesis system can be ascribed to the efficient transfer of the long-lived electrons from defective meso-Al_2O_3 to *E. coli* for powering the MVA pathway. Moreover, the hybrid meso-Al_2O_3/*E. coli* photo-biosynthesis system can produce farnesene with the productivity of 1220 mg/L

3

RESEARCH ARTICLE

under simulated solar light illumination (Figure S11), indicating that the hybrid photo-biosynthesis system is capable of converting solar energy into fine chemicals. Collectively, these results demonstrated that defects can be readily introduced in materials by porous structure to prolong the lifetime of photo-excited electrons, and the long-lived electrons can be transferred to the biosynthetic pathways in microorganisms to accelerate the production of fine chemicals.

The defects-mediated long-lived electrons in Al_2O_3 were further investigated with density functional theory (DFT) calculations at the atomic level. Different types of defects in Al_2O_3 were studied to investigate their role in charge separation regarding the total density of states (TDOSs). The common point defects including oxygen vacancy (V_O), interstitial oxygen (O_i), Al vacancy (V_{Al}) and interstitial Al (Al_i) were systematically investigated (Figure S12). Defects can act as traps to suppress charge recombination and prolong the lifetime of photo-excited electrons.[16] The TDOS results show that the charged oxygen vacancy can supply empty states to trap electrons (Figure S12a), and the Al vacancies also

contribute to the generation of long-lived electrons due to the multi electron-hole pair for energy trapping (Figure S12c). Furthermore, since large quantities of both Al and O vacancies exist in the meso-Al_2O_3, Schottky defects can easily form. The Schottky defects are a common type of defect that affects materials' electronic and optical properties. In this study, the Schottky defects were investigated in agglomerated and separated types. Figure 3a shows that large amounts of additional electronic and hole states are induced by the agglomerated Schottky defects. For instance, in the case of neutral V_{Al2O3}^0 (1), all the induced gap states are symmetrical, including three pairs of electronic states in 0.98, 1.45, and 2.16 eV (the upper panel) above the valence band maximum and one pair of localized hole states in 4.37 eV above the highest electronic state. Moreover, the separated Schottky defects induce even more gap states in the bandgap, as demonstrated in Figure 3b. The negatively charged Schottky defects significantly affect the electronic structures with abundant asymmetrical gap states near the mid-gap. The single-particle levels of the native point defects and Schottky defects with
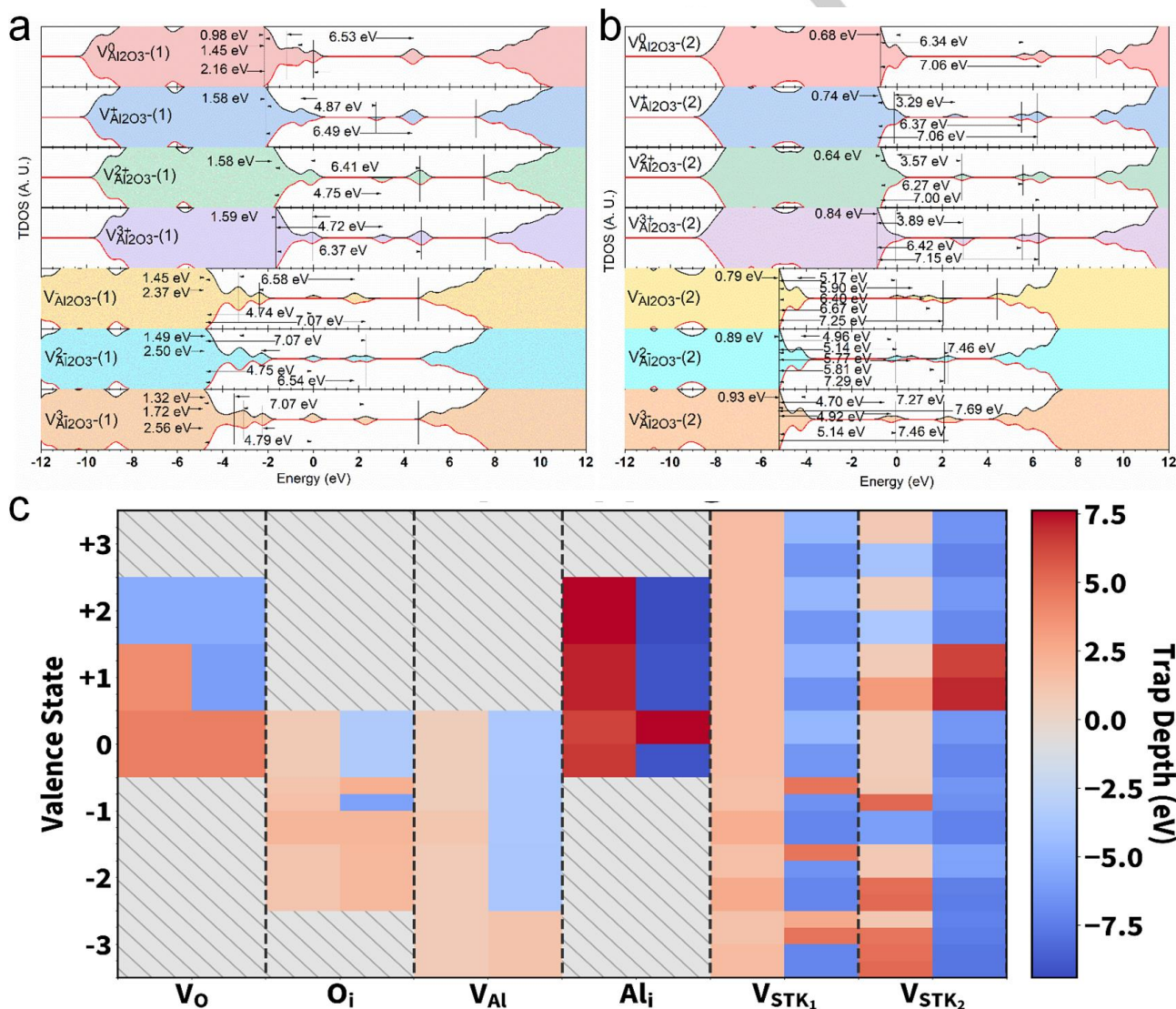

Figure 3. The origin of long-lived electrons in defective mesoporous Al_2O_3 (meso-Al_2O_3). (a) The total density of states (TDOSs) of agglomerated Schottky defect of Al_2O_3 from triply negative V_{Al2O3}^{3-} to triply positive V_{Al2O3}^{3+}. (b) TDOSs of separated Schottky defect of Al_2O_3 from triply negative V_{Al2O3}^{3-} to triply positive V_{Al2O3}^{3+}. (c) Summarized single-particle levels of intrinsic defects in Al_2O_3 with different charge states (empty states = negative value, filled states = positive value). V_O, oxygen vacancy; O_i, interstitial oxygen (O_i); V_{Al}, Al vacancy; Al_i, interstitial Al; V_{STK1}, agglomerated Schottky vacancy; V_{STK2}, separated Schottky vacancy.

RESEARCH ARTICLE

different charge states are further summarized in Figure 3c. Due to the extra-large intrinsic optical bandgap, the emission decay of the electronic inter-level transition is usually too short for Al_2O_3. However, by artificially creating the native defects in the material, the energetic interval between occupied (electronic) and unoccupied (hole) long-lifetime levels is significantly alleviated. Compared to the simple point defects, Schottky defects are more promising in prolonging the electron lifetime in defective meso-Al_2O_3 because Schottky defects can provide abundant localized electronic and hole states. The DFT calculations confirm that creating defects is an efficient strategy to prolong the lifetime of the photo-excited electrons in semiconductors.

The possible proteins by which the electrons from defective meso-Al_2O_3 passed to *E. coli* were further investigated. The direct attachment of *E. coli* to the defective meso-Al_2O_3 is observed in the scanning electron microscopy (SEM) image (Figure 4a). The binding of *E. coli* to meso-Al_2O_3 can be ascribed to the electrostatic interaction between the negatively charged *E. coli* and the positively charged meso-Al_2O_3 (Figure S13).[10,12a,21] According to previous studies, the attachment of *E. coli* to defective meso-Al_2O_3 is beneficial for electron transfer from defective meso-Al_2O_3 to *E. coli*.[12a,14] Electrically conductive c-type cytochrome and pilin have been proposed as efficient pathways for electrons transfer between contacted microorganisms.[11b] Considering the attachment of *E. coli* to defective meso-Al_2O_3, electron transfer from defective meso-Al_2O_3 to *E. coli* via c-type cytochrome or pilin may exist in the farnesene biosynthesis system. To verify this point, the genes

encoding c-type cytochrome and pilin were knockout in farnesene-producing *E. coli* strains, respectively (Figures S14 and S15).[22] As indicated in Figure 4b, in c-type cytochrome-deficient *E. coli* (Δccm), the produced farnesene is about 400 g/L in the presence of meso-Al_2O_3 and light illumination, which is less than a quarter of the farnesene produced in the hybrid meso-Al_2O_3/*E. coli* system. The significantly decreased production of farnesene indicates that the electrons of defective meso-Al_2O_3 cannot be efficiently passed to *E. coli* without c-type cytochrome, demonstrating that c-type cytochrome is essential in the transfer of electrons from defective meso-Al_2O_3 to *E. coli*. Similarly, the pilin-deficient *E. coli* ($\Delta FimA$) treated with defective meso-Al_2O_3 and light illumination also produced much less farnesene than the hybrid meso-Al_2O_3/*E. coli* system (Figure 4c). Additionally, nitazoxanide (NTZ), an antiparasitic drug shown to inhibit the aggregative adherence function of pili,[23] was applied to the hybrid photo-biosynthesis system to block pili. With the addition of NTZ, the production of farnesene in the hybrid photo-biosynthesis system falls by more than half (Figure S16), again confirming that the electrons in defective meso-Al_2O_3 cannot be efficiently passed to *E. coli* in the dysfunction of pilin. These results thus provide evidence that the long-lived electrons in defective meso-Al_2O_3 cannot be efficiently transferred to *E. coli* in the absence of c-type cytochrome or pilin, suggesting that c-type cytochrome and pilin play crucial roles in passing the electrons from meso-Al_2O_3 to *E. coli* (Figure 4d).

The MVA pathway for farnesene production involves the conversion of acetyl-CoA into MVA, geranyl pyrophosphate, and farnesyl pyrophosphate. Farnesene is further biosynthesized by using geranyl pyrophosphate (GPP) and farnesyl pyrophosphate (FPP) as the building blocks (Figure 5a).[2b] The performance of the hybrid photo-biosynthesis system in farnesene production was further investigated. The concentrations of the GPP and FPP in the hybrid photo-biosynthesis system are found to be lower compared to bare *E. coli*. Whereas, significantly elevated production of farnesene in the hybrid photo-biosynthesis system is observed (Figure 5b), which can be attributed to the accelerated consumption of GPP and FPP in the hybrid photo-biosynthesis system for farnesene overproduction. Figure 5c further shows that the NADPH/NADP$^+$ ratio in the hybrid photo-biosynthesis system is more than two times that of the bare farnesene producing *E. coli*, showing that the light-harvesting meso-Al_2O_3 can efficiently convert light energy into NADPH. The farnesene production kinetics further shows that the yield of farnesene in the hybrid photo-biosynthesis system increases rapidly within the first 24 h and begins to plateau after 72 h of reaction (Figure 5d), which can be ascribed to the gradual slowing down of bacterial growth in the photo-biosynthesis system after 72 h. Compared to the hybrid photo-biosynthesis system, the meso-Al_2O_3/*E. coli* group in dark produces much less farnesene over time, suggesting that the hybrid photo-biosynthesis system is efficient in solar-to-chemical synthesis. The viability of *E. coli* in the hybrid photo-biosynthesis system was also investigated by measuring the OD_{600} and cell number. The OD_{600} and the counted cell number rapidly increase within 24 h (Figure 5e), indicating the rapid proliferation of *E. coli* in the presence of meso-Al_2O_3 and light illumination. The bare farnesene producing *E. coli* displays a similar growth curve to the *E. coli* in the hybrid photo-biosynthesis system (Figures S17 and S18), indicating that the defective meso-Al_2O_3 exhibit excellent biocompatibility with microorganisms. Taken together, the defective meso-Al_2O_3 can provide long-lived electrons for fine
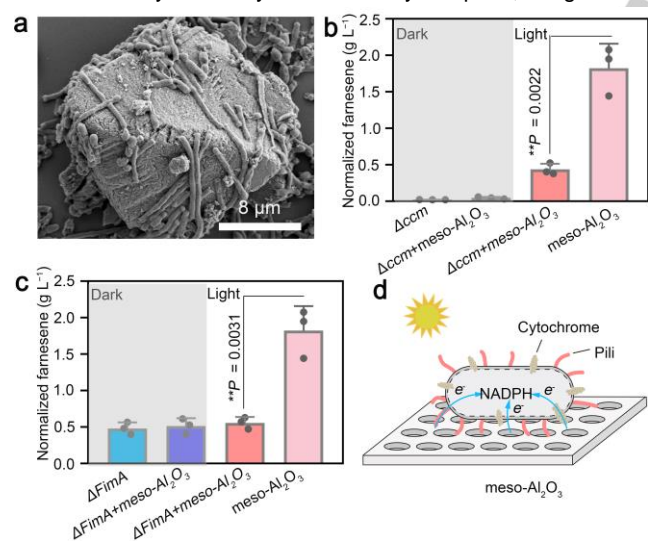
Figure 4. Electron transfer from mesoporous Al_2O_3 (meso-Al_2O_3) to *E. coli*. (a) Scanning electron microscopy image of the meso-Al_2O_3/*E. coli*. (b) The yield of farnesene production in c-type cytochrome-deficient *E. coli* (Δccm, dark), c-type cytochrome-deficient *E. coli* treated with defective meso-Al_2O_3 (Δccm + meso-Al_2O_3, dark), c-type cytochrome-deficient *E. coli* treated with defective meso-Al_2O_3 and illumination (Δccm + meso-Al_2O_3, light), and the original hybrid meso-Al_2O_3/*E. coli* system (meso-Al_2O_3, light). (c) The yield of farnesene production in pilin-deficient *E. coli* ($\Delta FimA$, dark), pilin-deficient *E. coli* treated with meso-Al_2O_3 ($\Delta FimA$ + defective meso-Al_2O_3, dark), pilin-deficient *E. coli* treated with defective meso-Al_2O_3 and illumination ($\Delta FimA$ + meso-Al_2O_3, light), and the original hybrid meso-Al_2O_3/*E. coli* system (meso-Al_2O_3, light). (d) Schematic illustration showing the transfer of electrons from defective meso-Al_2O_3 to *E. coli*. Pilin is the conductive protein on the pili of *E. coli*. NADPH, reduced nicotinamide adenine dinucleotide phosphate. Error bars show the mean ± standard error of the mean (s.e.m.) of three independent measurements.
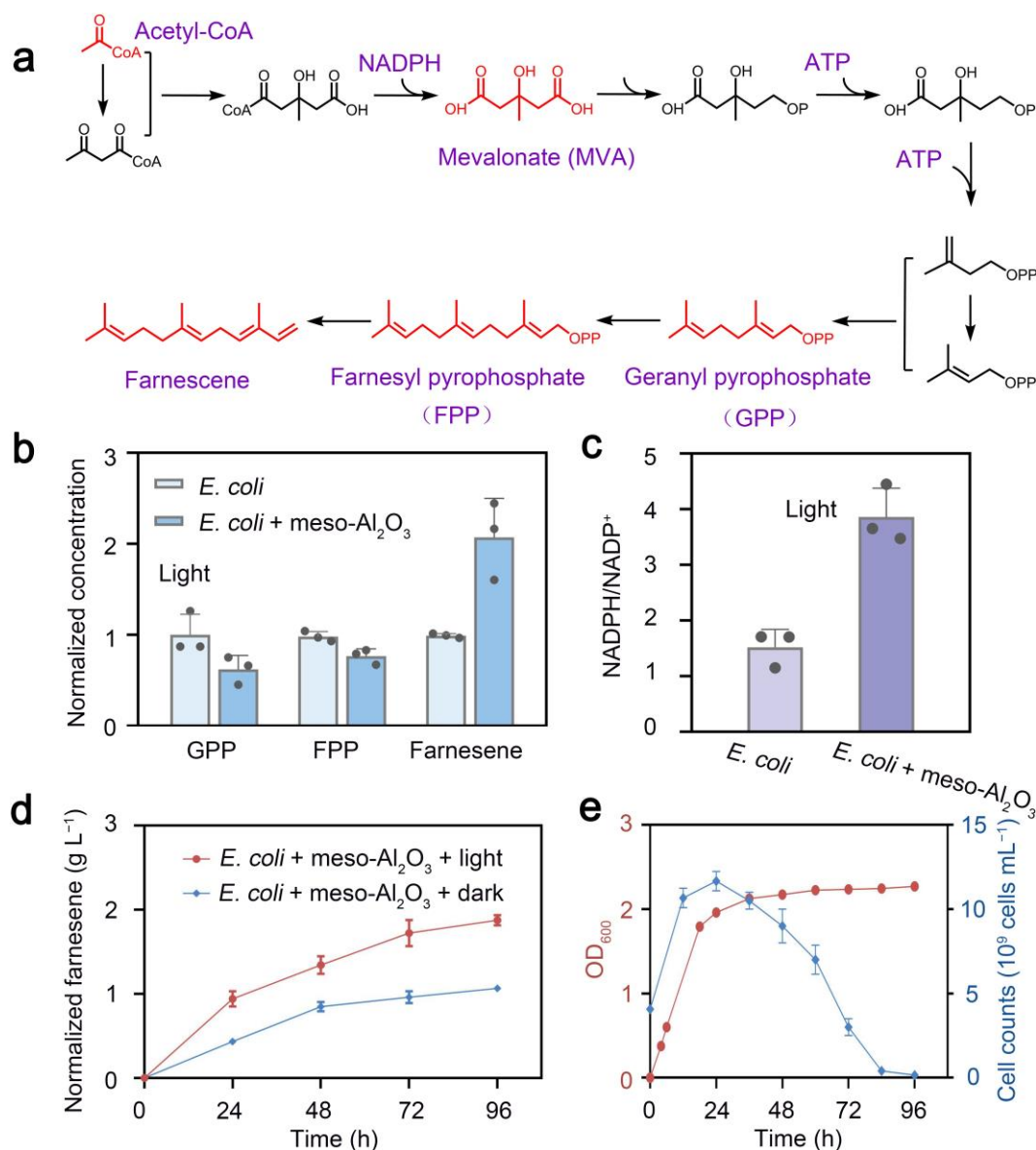
Figure 5. Farnesene production in the hybrid photo-biosynthesis system. (a) The mevalonate (MVA) pathway for farnesene production. NADPH, reduced nicotinamide adenine dinucleotide phosphate; ATP, adenosine triphosphate. (b) The relative concentrations of geranyl pyrophosphate (GPP), farnesyl pyrophosphate (FPP), and farnesene in bare farnesene-producing *E. coli* and the hybrid photo-biosynthesis system. (c) The ratio of reduced nicotinamide adenine dinucleotide phosphate to nicotinamide adenine dinucleotide phosphate (NADPH/NADP$^+$) in bare *E. coli* and the hybrid photo-biosynthesis system. (d) Normalized concentration of farnesene produced by the hybrid biosynthesis system in light and dark over time. (e) The OD$_{600}$ of the hybrid photo-biosynthesis system and the counted cell numbers of *E. coli* in the system over time. Error bars show the mean ± standard error of the mean (s.e.m.) of three independent measurements.

chemical production, showing its good promise in solar-to-chemical synthesis with microbial cell factories.

Conclusion

In summary, we have demonstrated that the lifetime of photo-excited electrons in semiconductors can be prolonged by creating defects, and the long-live electrons can be efficiently transferred to microorganisms to power the biosynthetic pathways for fine chemical production in high yields. By constructing a highly porous structure in Al$_2$O$_3$, the amounts of defects were largely increased and the lifetime of photo-excited electrons was significantly prolonged. With the assistance of the long-lived electrons in meso-Al$_2$O$_3$, the yield of farnesene production in *E.*

coli was increased from about 900 mg/L to 1816 mg/L under visible light illumination. Additionally, the c-type cytochrome and pilin were demonstrated to participate in the electron transfer process in the photo-biosynthesis system. The method developed in this work can not only open new possibilities for prolonging the lifetime of photo-excited electrons in solid materials but also provide further avenues to elevate the production yields of fuels, pharmaceuticals and other high-value chemicals in microbial cell factories with solar energy.

Acknowledgments

6

RESEARCH ARTICLE

[1] a) J. Nielsen, J. D. Keasling, *Cell* **2016**, *164*, 1185-1197; b) A. S. Khalil, J. J. Collins, *Nat. Rev. Genet.* **2010**, *11*, 367-379; c) A. L. Meadows, K. M. Hawkins, Y. Tsegaye, E. Antipov, Y. Y. Kim, L. Raetz, R. H. Dahl, A. Tai, T. Mahatdejkul-Meadows, X. Lan, L. S. Zhao, M. S. Dasika, A. Murarka, J. Lenihan, D. Eng, J. S. Leng, C. L. Liu, J. W. Wenger, H. X. Jiang, L. Chao, P. Westfall, J. Lai, S. Ganesan, P. Jackson, R. Mans, D. Platt, C. D. Reeves, P. R. Saija, G. Wichmann, V. F. Holmes, K. Benjamin, P. W. Hill, T. S. Gardner, A. E. Tsong, *Nature* **2016**, *537*, 694–697; d) C. J. Paddon, J. D. Keasling, *Nat. Rev. Microbiol.* **2014**, *12*, 355-367.

[2] a) P. P. Peralta-Yahya, F. Zhang, S. Cardayre, J. D. Keasling, *Nature* **2012**, *488*, 320-328; b) M. Chang, J. D. Keasling, *Nat. Chem Biol.* **2006**, *2*, 674-681; c) Q. L. Liu, T. Yu, X. W. Li, Y. Chen, Y. Chen, K. Campbell, J. Nielsen, Y. Chen, *Nat. Commun.* **2019**, *10*, 4976; d) T. Ma, B. Shi, Z. L. Ye, X. W. Li, M. Liu, Y. Chen, J. Xia, J. Nielsen, Z. X. Deng, T. G. Liu, *Metab. Eng.* **2019**, *52*, 134-142.

[3] a) D. W. Christianson, *Science* **2007**, *316*, 60-61; b) G. K. Bian, Z. X. Deng, T. T. Liu, *Curr. Opin. Biotech.* **2017**, *48*, 234-241.

[4] a) C. J. Paddon, P. J. Westfall, D. J. Pitera, K. Benjamin, K. Fisher, D. McPhee, M. D. Leavell, A. Tai, A. Main, D. Eng, D. R. Polichuk, K. H. Teoh, D. W. Reed, T. Treynor, J. Lenihan, M. Fleck, S. Bajad, G. Dang, D. Diola, G. Dorin, K. W. Ellens, S. Fickes, J. Galazzo, S.P. Gaucher, T. Geistlinger, R. Henry, M. Hepp, T. Horning, T. Iqbal, H. Jiang, L. Kizer, B. Lieu, D. Melis, N. Moss, R. Regentin, S. Secrest, H. Tsuruta, R. Vazquez, L. F. Westblade, L. Xu, M. Yu, Y. Zhang, L. Zhao, J. Lievense, P. S. Covello, J. D. Keasling, K. K. Reiling, N. S. Renninger, J. D. Newman, *Nature* **2013**, *496*, 528-532; b) V. J. J. Martin, D. J. Pitera, S. T. Withers, J. D. Newman, J. D. Keasling, *Nat. Biotechnol.* **2003**, *21*, 796-802.

[5] F. Y. Zhu, X. F. Zhong, M. Z. Hu, L. Liu, Z. X. Deng, T. G. Liu, *Biotechnol. Bioeng.* **2014**, *111*, 1396-1405.

[6] S. Y. Lee, H. U. Kim, T. U. Chae, J. S. Cho, J. W. Kim, J. H. Shin, D. I. Kim, Y. S. Ko, W. D. Jang, Y. S. Jang, *Nat. Catal.* **2019**, *2*, 18-33.

[7] a) X. D. Wang, T. Saba, H. H. P. Yiu, R. F. Howe, J. A. Anderson, J. F. Shi, *Chem* **2017**, *2*, 621-654; b) S. K. Spaans, R. A. Weusthuis, V. John, S. Kengen, *Front. Microbiol.* **2015**, *6*, 742.

[8] J. S. Cho, S. H. PARK, H. U. Kim, T. Y. Kim, J. S. Park, H. Chung, S. Y. Lee, *Nat. Commun.* **2014**, *5*, 4618.

[9] a) S. Y. Kim, J. Lee, S. Y. Lee, *Biotechnol. Bioeng.* **2015**, *112*, 416-421; b) Y. J. Zhou, E. J. Kerkhoven, N. Jens, *Nat. Energy* **2018**, *3*, 925-935.

[10] J. L. Guo, M. Suastegui, K. K. Sakimoto, V. M. Moody, G. Xiao, D. G. Nocera, N. S. Joshi, *Science* **2018**, *362*, 813-816.

[11] a) K. Rabaey, R. A. Rozendal, *Nat Rev Microbiol.* **2010**, *8*, 706-716; b) Q. D. Yin, G. X. Wu, *Biotechnol. Adv.* **2019**, *37*, 107443.

[12] a) K. K. Sakimoto, A. B. Wong, P. D. Yang, *Science* **2016**, *351*, 74-77; b) H. Zhang, H. Liu, Z. Q. Tian, D. Lu, Y. Yu, S. Cestellos-Blanco, K. K. Sakimoto, P. D. Yang, *Nat. Nanotechnol.* **2018**, *13*, 900-905.

[13] a) R. Chen, F. D. Fan, D. Thomas, C. Li, *Chem. Soc. Rev.* **2018**, *47*, 8238-8262; b) N. Zhang, C. Gao, Y. J. Xiong, *J. Energy Chem.* **2019**, *37*, 55-69.

[14] K. K. Sakimoto, N. Kornienko, S. Cestellos-Blanco, J. Lim, C. Liu, P. D. Liu, *J. Am. Chem. Soc.* **2018**, *140*, 1978-1985.

[15] X. H. Liu, F. Y, Kang, H. Cheng, L. Wang, X. Zhen, D. D. Zheng, W. M. Gong, Y. Lu, Y. H. Ma, J. Y. Wang, *Nat. Chem.* **2018**, *10*, 1201-1206.

[16] a) G. Ou, Y. S. Xu, B. Wen, R. Lin, B. H. Ge, Y. Tang, Y. W. Liang, C. Yang, K. Huang, D. Zu, R. Yu, W. X. Chen, J. Li, H. Wu, L. M. Liu, Y. D. Li, *Nat. Commun.* **2018**, *9*,1302; b) Q. Q. Ma, W. Jie, Z. Wei, Q. Wang, Q. Yuan, *Sci. China: Chem.* **2018**, *61*, 1624-1629; c) J. Wang, Q. Q. Ma, Y. Q. Wang, H. J. Shen, Q. Yuan, *Nanoscale* **2017**, *61*, 6204-6218.

[17] Q. Yuan, A. X. Yin, C. Luo, L. D. Sun, Y. W. Zhang, W. T. Duan, H. C. Liu, C. H. Yan, *J. Am. Chem. Soc.* **2008**, *130*, 3465-3472.

[18] a) X. Zhang, B. Xiong, J. Li, L. Qian, C. He, *ACS Appl. Mater. Interfaces* **2019**, *11*, 31441-31451; b) J. Kansy, *Nucl. Instrum. Methods Phys. Res.* **1996**, *374*, 235-244.

[19] D. V. Ananchenko, S. V. Nikiforov, S. F. Konev, G. R. Ramazanova, *Opt. Mater.* **2019**, *90*, 118-122.

[20] a) L. El. Mira, A. Amlouka, C. Barthou, *J. Phys. Chem. Solids* **2006**, *67*, 2395-2399; b) G. P. Williams, G. H. Rosenblatt, M. J. Ferry, R. T. Williams, Y. Chen, *J. Lumin.* **1988**, 40-41, 339-340.

[21] a) J. Z. Pan, G. D. Gong, Q. Wang, J. J. Shang, Y. X. He, C. Catania, D. Birnbaum, Y. F. Li, Z. J. Jia, Y. Y. Zhang, N. S. Joshi, J. L. Guo, *Nat. Commun.* **2022**, *13*, 2117; b) Z. M. Zhao, D. C. Pan, Q. M. Qi, J. Kim, N. Kapate, T. Sun, C. W. S. IV, L. L. Wang, D. Wu, C. J. Kwon, W. He, J. L. Guo, S. Mitragotri, *Adv. Mater.* **2020**, *32*, 2003492.

[22] a) R. Schmidt, A. Krizsan, D. Volke, D. Knappe, R. Hoffmann, *J. Proteome Res.* **2016**, *15*, 2607-2617; b) C. L. Richard-Fogal, B. S. Francisco, E. R. Frawley, R. G. Kranz, *Biochim. Biophys. Acta, Bioenerg.* **2012**, *1817*, 911-919.

[23] P. Chahales, P. S. Hoffman, D. G. Thanassi, Antimicrob. *Agents Chemother.* **2016**, *60*, 2028-2038.

WILEY-VCH

RESEARCH ARTICLE

Entry for the Table of Contents
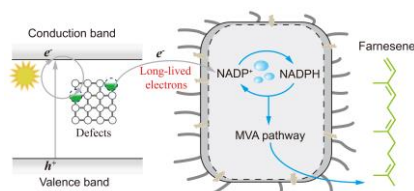
A hybrid photo-biosynthesis system was constructed for the overproduction of jet fuel farnesene by interfacing engineered *E. coli* with persistent phosphor mesoporous Al$_2$O$_3$ (meso-Al$_2$O$_3$). Meso-Al$_2$O$_3$ with rich defects prolonged the lifetime of photo-excited electrons that were passed to *E. coli* and improved the farnesene production by a factor of over 100%.

Jie Wang, Na Chen, Guangkai Bian, Xin Mu, Na Du, Wenjie Wang, Chong-Geng Ma, Shai Fu, Bolong Huang, Tiangang Liu, Yanbing Yang, Quan Yuan

Page No. – Page No.

Solar-driven Overproduction of Biofuels in Microorganisms